Available online at www.sciencedirect.com

ScienceDirect

Neuromuscular Disorders 29 (2019) 274–281

www.elsevier.com/locate/nmd

Comparative transcriptome analysis of skeletal muscle in ADSSL1 myopathy

Hyung Jun Park[a,b,1], Ji-Man Hong[b,1], Jung Hwan Lee[c], Ha Young Shin[b], Seung Min Kim[b], Kee Duk Park[c], Ji Hyun Lee[d,e,*], Young-Chul Choi[b,**]

[a] Department of Neurology, Gangneung Asan Hospital, University of Ulsan College of Medicine, Gangneung, Republic of Korea
[b] Department of Neurology, Gangnam Severance Hospital, Yonsei University College of Medicine, 211 Eonju-ro, Gangnam-gu, Seoul, Republic of Korea
[c] Department of Neurology, Mokdong Hospital, Ewha Womans University School of Medicine, Seoul, Republic of Korea
[d] Department of Clinical Pharmacology and Therapeutics, College of Medicine, Kyung Hee University, Dongdaemun-gu, Kyung Hee daero 26, Seoul, Republic of Korea
[e] Kyung Hee Medical Science Research Institute, Kyung Hee University, Seoul, Republic of Korea

Received 2 August 2018; received in revised form 7 November 2018; accepted 14 November 2018

Abstract

ADSSL1 myopathy was recently identified as the cause of muscular disorders in Korean patients with distal myopathy. We generated transcriptome profiles of muscles from control subjects and patients with ADSSL1 myopathy. In the present study, RNA sequencing was conducted with seven vastus lateralis muscle samples from four patients with ADSSL1 myopathy and three control subjects. The hierarchical clustering result revealed a separation between myopathy and control groups. A total of 1,260 transcripts were significantly differentially expressed ($|\text{fold change}| \geq 2$, $p < 0.05$), with 740 upregulated transcripts and 520 downregulated transcripts in myopathy group. Eighteen transcripts that mapped to purine metabolism pathway were significantly differentially expressed between the two groups, with ten downregulated transcripts and eight upregulated transcripts in myopathy group. In particular, three genes involved in purine nucleotide cycle (*ADSSL1*, *ADSL*, and *AMPD1*) were significantly downregulated in myopathy group. Ten transcripts in glycolysis/gluconeogenesis pathway were also significantly differentially expressed. This is the first study on the altered expression of transcripts in muscle tissues from patients with ADSSL1 myopathy. Our results provide new insights into the pathogenesis of ADSSL1 myopathy.

Keywords: RNA-Seq; Transcriptome; Gene expression; ADSSL1; Pathomechanism; Myopathy.

1. Introduction

Distal myopathy is a clinically and genetically heterogeneous group of genetic muscle disorders characterized by progressive muscular weakness beginning in the foot and hand muscles. Eighteen genes associated with distal myopathy have been identified [1]. Among them, *ADSSL1* was recently identified as the causative gene of distal myopathy [2]. Clinical presentation of ADSSL1 myopathy includes predominant distal leg involvement, mild facial weakness, and mildly elevated creatine kinase (CK) level [2–4]. Muscle pathology mainly revealed non-specific chronic myopathic change, but rarely showed rimmed vacuoles or nemaline bodies [2,4]. Muscle magnetic resonance imaging (MRI) showed predominant fatty replacements and muscle atrophy in distal limb and tongue muscles [4]. However, ADSSL1 myopathy has been reported in only a few Korean patients and its pathomechanism remains unclear.

RNA sequencing (RNA-Seq) analyzes the presence and quantity of complementary DNAs (cDNAs) using next-generation sequencing [5]. It provides a comprehensive understanding of alternative gene spliced transcripts, post-transcriptional modifications, gene fusions, single

* Corresponding author at: Department of Clinical Pharmacology and Therapeutics, College of Medicine, Kyung Hee University, Dongdaemun-gu, Kyung Hee daero 26, Seoul, Republic of Korea.
** Corresponding author.
E-mail addresses: hyunihyuni@khu.ac.kr (J.H. Lee), ycchoi@yuhs.ac (Y.-C. Choi).
[1] Both authors contributed equally to this work.

https://doi.org/10.1016/j.nmd.2018.11.003
0960-8966/

Table 1
Clinical presentation of ADSSL1 myopathy patients and control subjects.

Subject	Sex	*ADSSL1* mutations	Age at exam, year	Age at onset, year	Clinical presentation	CK, IU/l	Muscle pathology	Biopsy site	Ref
II-2 in FC628	M	c.910G > A + c.1048delA	31	8	Diffuse muscle weakness initially, followed by ankle dorsiflexor weakness	365	Rimmed vacuoles	VL	[2]
II-2 in MF1184	F	c.910G > A + c.1048delA	15	8	Diffuse muscle weakness, followed by ankle dorsiflexor weakness	281	Rimmed vacuoles	VL	[3]
II-1 in MF650	M	c.910G > A + c.1048delA	32	7	Diffuse muscle weakness initially, followed by distal muscle weakness in adolescence and quadriceps muscle weakness in the early 30s	431	Nemaline rods	VL	[4]
II-1 in MF578	M	c.910G > A + c.1048delA	29	5	Diffuse muscle weakness initially, followed by ankle dorsiflexor weakness	420	Chronic myopathy	VL	[4]
Control 1	F	–	16	–	Psychogenic weakness	54	Normal	VL	–
Control 2	F	–	47	–	Cramp	34	Normal	VL	–
Control 3	M	–	14	–	Psychogenic weakness	137	Normal	VL	–

CK, creatine kinase; VL, vastus lateralis muscle.

nucleotide variations, and changes in gene expression. RNA-Seq also allows mapping of exon/intron boundaries and the identification of annotated 5′ and 3′ gene boundaries. In particular, different expression levels between affected and healthy groups can reveal cellular changes associated with disease status and suggest the pathomechanism. RNA-Seq has been used to identify gene drivers and pathomechanism in various cancers, chronic diseases, and genetic diseases [6–8]. To understand the transcriptomic signature and propose the pathomechanism of ADSSL1 myopathy, we generated and compared transcriptome profiles of muscles from control subjects and patients with ADSSL1 myopathy.

2. Materials and methods

2.1. Study subjects

For the present study, we reviewed medical records of the myopathy database from January 2002 to October 2016. Seven vastus lateralis muscle samples from four patients with ADSSL1 myopathy (II-2 in FC628, II-1 in MF578, II-1 in MF650, and II-2 in MF1184) and three control subjects (MF592, MF1046, and MF1213) were enrolled in this study. The four patients with ADSSL1 myopathy were genetically confirmed and previously reported [2–4]. Table 1 summarized the clinical and laboratory spectrum of study subjects. The patients with ADSSL1 myopathy had the same compound heterozygous pathogenic variants in the *ADSSL1* gene (c.910G > A + c.1048delA). For the selection of control subjects, we identified three individuals who fulfilled the following criteria: (i) normal muscle pathology, (ii) normal serum creatine kinase level, (iii) without definite muscle weakness, and (iv) available vastus lateralis muscle biopsy samples. Among them, two subjects (MF592 and MF1213) were finally diagnosed with psychogenic weakness and one (MF1046) was diagnosed with muscle cramp. The institutional review board of Gangnam Severance hospital, Korea, approved the research protocol (IRB No. 3-2016-0304). All participants provided informed consent for genetic analysis.

2.2. RNA-Seq data

cDNA libraries were constructed with the TruSeq RNA library kit using 1 μg of total RNA. The protocol consisted of polyA-selected RNA extraction, RNA fragmentation, random hexamer-primed reverse transcription, and 100-nt paired-end sequencing by Illumina HiSeq2500. The libraries were quantified using quantitative polymerase chain reaction (qPCR) according to the qPCR Quantification Protocol Guide and qualified using an Agilent Technologies 2100 Bioanalyzer. We processed reads from the sequencer and aligned them to the hg19 reference genome using Tophat v2.0.13 [9]. Tophat incorporates the Bowtie v2.2.3 algorithm to perform the alignment. Tophat initially removes a portion of the reads based on the quality information accompanying each read before it maps reads to the reference genome. The reference genome and annotation data were downloaded from the UCSC table browser (http://genome.uscs.edu). Gene annotation information also was used for running Tophat with "-G" option. Default options were used for other parameters. Tophat allows multiple alignments per read (up to 20 by default) and a maximum of two mismatches when mapping the reads to the reference. Transcript assembly and abundance estimation was performed using Cufflinks [10]. After aligning reads to the genome, Cufflinks v2.2.1 was used to assemble aligned reads into transcripts and to estimate their abundance. To correct sequence expression count bias, '–max-bundle-

frags 50,000,000' options were used. We also employed the '-G' option to make the best use of known gene annotation information. Default options were used for other parameters. These raw reads were deposited into the NCBI Sequence Read Archive (SRA) database (Accession Number: SRP149027).

2.3. Statistical analysis of gene expression level

The transcript counts at the isoform level were calculated and relative transcript abundance was measured in fragments per kilobase of exon per million fragments mapped (FPKM) from Cufflinks. FPKM is calculated as ($10^9 \times$ the number of mappable exon reads) / (the total number of mappable reads $\times$ the number of base pairs in the exon). To facilitate log2 transformation, 1 was added to each FPKM value of filtered genes. Filtered data were log2-transformed and subjected to quantile normalization. Statistical significance of the differential expression data was determined using independent *t*-test and fold change; the null hypothesis was that no difference exists among groups. False discovery rate (FDR) was controlled by adjusting the p value using the Benjamini-Hochberg algorithm. Hierarchical clustering analysis was performed using complete linkage and Euclidean distance as a measure of similarity to display the expression patterns of differentially expressed genes (DEGs) that satisfied the criteria of $|\text{fold change}| \geq 2$ and independent *t*-test raw $p < 0.05$. Gene-enrichment and functional annotation analysis for the significant gene list was performed using Gene Ontology (www.geneontology.org/), and pathway analysis for the DEG was performed based on KEGG pathways (http://www.genome.jp/kegg/pathway.html).

2.4. Volume plot

Expression volume is defined as the geometric mean of the expression level for the two groups. To confirm the genes that show higher expression difference compared to the control according to expression volume, a volume plot was drawn in which the X-axis represented volume and the Y-axis represented log2 fold change. For example, even though the fold change might be different by two-fold for two genes, the gene with a higher volume may be more credible.

2.5. Quantitative reverse-transcription PCR (qRT-PCR)

Validation of RNA-Seq gene expression profiling results was performed for three genes involved in purine nucleotide cycle (*ADSSL1*, *ADSL,* and *AMDP1*) and one housekeeping gene (*GAPDH*). All primer sets are listed in Supplementary Table 1. Total RNA extracted from skeletal muscles was reverse transcribed using a RevertAid First Strand cDNA synthesis kit (Thermo Fisher Scientific Inc., Waltham, MA, USA). The relative amounts of mRNA were estimated in duplicate samples by fluorescence and quantified using an ABI 7300 Real-Time PCR system (Applied Biosystems, Foster City, CA). The reaction was initiated in a total volume of 20 μL containing 10 ng of cDNA and 1pM of each primer in a reaction buffer containing $2 \times$ QPCR Green Master Mix HRox (Biotech rabbit, Hennigsdorf, Germany). The cycle threshold (Ct) values were normalized against *GAPDH* gene expression. The results were expressed as target gene expression relative to control gene expression. PCR amplification was performed with initial denaturation for 2 min at 95 °C followed by 40 cycles of amplification (15 s at 95 °C and 30 seconds at 60 °C) with the same primer sets as used for qRT-PCR.

2.6. Histological examination of muscle specimens

Histopathological analyses of the vastus lateralis muscles were performed in all patients. Frozen 10-μm sections were examined by staining with hematoxylin and eosin (H&E), modified Gomori trichrome (modified GT), nicotinamide adenine dinucleotide tetrazolium reductase (NADH-tr), and myosin ATPase preincubated at pH 4.3, 4.6, and 9.4. Histopathologic studies on myopathy group showed chronic myopathic features, and were previously reported [2–4]. However, three control subjects showed normal muscle pathology. We analyzed the proportions of type I and type II muscle fibers through comparison with muscle histology to find evidence of an association between ADSSL1 deficiency and abnormal glycolysis/gluconeogenesis pathway.

2.7. Non-ischemic forearm test

We performed non-ischemic forearm test in II-1 patient in MF650. He squeezed the handgrip dynamometer at intended maximal voluntary contraction during each contraction (contraction, 1 s; rest, 1 s). The exercise lasted for 1 minute, and it was performed without blocked blood circulation. Blood samples were collected from the median cubital vein of exercising arm before exercise and after 1, 2, 4, 6, and 10 min to monitor lactate and ammonia.

2.8. Statistical analysis

Transcript divergence from the qRT-PCR results was evaluated for statistical significance using the Student's *t*-test. Differences were considered statistically significant at $p < 0.05$. All statistical analyses were conducted using R 3.1.2 (www.r-project.org).

3. Results

RNA-Seq was completed for vastus lateralis muscles from four patients with ADSSL1 myopathy and three control subjects. Initial quality assessment of the reads was performed using fastQC and all RNA-Seq data were judged to have high quality. The number of total reads, alterative splices, and putative novel isoforms per sample provided from RNA-sequencing is provided in Supplementary Table 2. There were no significant differences in sequencing depth or mapping efficiency between the two groups. Expression values were normalized to transcript assembly and abundance estimation

Table 2
Genes involved in purine metabolism that are significantly upregulated and downregulated with greater than two-fold change.

Gene symbol	Description	RNA-Seq fold change
AMPD1	adenosine monophosphate deaminase 1	−5.806831
ADSL	adenylosuccinate lyase	−2.456209
PDE4D	phosphodiesterase 4D, cAMP-specific	−2.362400
ENPP4	ectonucleotide pyrophosphatase/phosphodiesterase 4	−2.223105
NT5C2	5′-nucleotidase, cytosolic II	−2.172034
ADCY9	adenylate cyclase 9	−2.165729
NT5C1A	5′-nucleotidase, cytosolic IA	−2.121268
GMPR	guanosine monophosphate reductase	−2.112618
ADCY2	adenylate cyclase 2	−2.088349
PGM1	phosphoglucomutase 1	−2.039340
NUDT5	nudix (nucleoside diphosphate linked moiety X)-type motif 5	2.026779
HDDC3	HD domain containing 3	2.165370
IMPDH1	IMP (inosine 5′-monophosphate) dehydrogenase 1	2.196139
ITPA	inosine triphosphatase	2.303530
APRT	adenine phosphoribosyltransferase	2.410736
GUK1	guanylate kinase 1	2.501662
NME1	NME/NM23 nucleoside diphosphate kinase 1	2.662026
ADA	adenosine deaminase	2.962271

using Cufflinks and reported FPKM. For principle gene analysis, 9035 of 25,906 transcripts with zero FKRMs were excluded. Of the remaining 16,871 transcripts, 891 transcripts were upregulated (> 2 fold) and 613 transcripts were downregulated (< 2 fold) in myopathy group compared with control group.

The heat map for hierarchical clustering showed a separation between myopathy and control groups (Fig. 1A). However, one sample from II-2 patient of MF1184 showed slightly different cluster compared to other patients with ADSSL1 myopathy. When we reanalyzed transcriptome data set of six samples excluding II-2 patient of MF1184, the two results were not significantly different. The volume plot revealed the distribution of transcripts between myopathy and control groups (Fig. 1B). A comparison of gene expression in myopathy and control groups showed that a total of 1260 transcripts were significantly differentially expressed ($|\text{fold change}| \geq 2$, $p < 0.05$), with 740 upregulated transcripts and 520 downregulated transcripts in myopathy group.

The differentially expressed genes were categorized by gene ontology (GO). We identified 2840 enriched GO terms in myopathy versus control group (FDR-adjusted p-value < 0.05). Top 20 KEGG pathways of DEGs in ADSSL1 myopathy were metabolic pathways, biosynthesis of antibiotics, carbon metabolism, biosynthesis of amino acids, pentose phosphate pathway, glycolysis/gluconeogenesis, cytokine-cytokine receptor interaction, cell adhesion molecules, calcium signaling pathway, cGMP-PKG signaling pathway, MAPK signaling pathway, cAMP signaling pathway, AMPK signaling pathway, Hippo signaling pathway, phagosome, regulation of actin cytoskeleton, focal adhesion, endocytosis, and p53 signaling pathway (Supplementary Fig. 1). Among them, we focused on muscle energy metabolism, including purine metabolism, and glycolysis/gluconeogenesis pathways. Enrichment of the KEGG pathways reflected similar themes with significant enrichment of purine metabolism pathway (hsa00230) and glycolysis/gluconeogenesis pathway (hsa00010). Eighteen genes that mapped to the KEGG pathway involved with "purine metabolism" were significantly differentially expressed between the two groups. Ten transcripts (*AMPD1, ADSL, PDE4D, ENPP4, NT5C2, ADCY9, NT5C1A, GMPR, ADCY2*, and *PGM1*) were significantly downregulated, and eight genes (*NUDT5, HDDC3, IMPDH1, ITPA, APRT, GUK1, NME1*, and *ADA*) were upregulated in myopathy group (Table 2). In particular, three genes involved in purine nucleotide cycle (*ADSSL1*, *ADSL* and *AMPD1*) were significantly downregulated in myopathy group (Fig. 2A). qRT-PCR data validated significant downregulation of *ADSSL1*, *ADSL*, and *AMPD1* transcripts in myopathy group ($p = 0.0019$, $p = 0.0025$, and $p = 0.0015$ respectively; Fig. 1D). Ten genes linked to glycolysis/gluconeogenesis pathway were also differentially expressed between the two groups: five transcripts (*ENO3, ACSS2, PFKM, PGAM2,* and *PGM1*) were significantly downregulated and five transcripts (*ADH1B, PGAM1, ALDOC, ENO1*, and *PGAM4*) were significantly upregulated in myopathy group (Fig. 2B). However, four transcripts were significantly linked to fatty acid degradation pathway (hsa00071), which is another important muscle energy metabolism pathway: three transcripts (*ACAT1*, *ACADM*, and *ACADSB*) were downregulated and one transcript (*ADH1B*) was upregulated in myopathy group.

We analyzed muscle pathology and non-ischemic forearm test to find evidence of association between ADSSL1 deficiency and abnormal glycolysis/gluconeogenesis pathway. We analyzed the proportions of type I and type II muscle fibers by comparison with muscle histology. NADH-tr staining and ATPase staining at pH 9.4 showed predominance of type I fibers in myopathy group (85% in II-2 in FC628, 74% in II-2 in MF1184, 51.1% in II-1 in MF650, and 79% in II-1 in MF578) compared to control group (44% in control 1, 26% in control 2, and 43% in control 3). Non-ischemic forearm test performed in II-1 in MF650 did

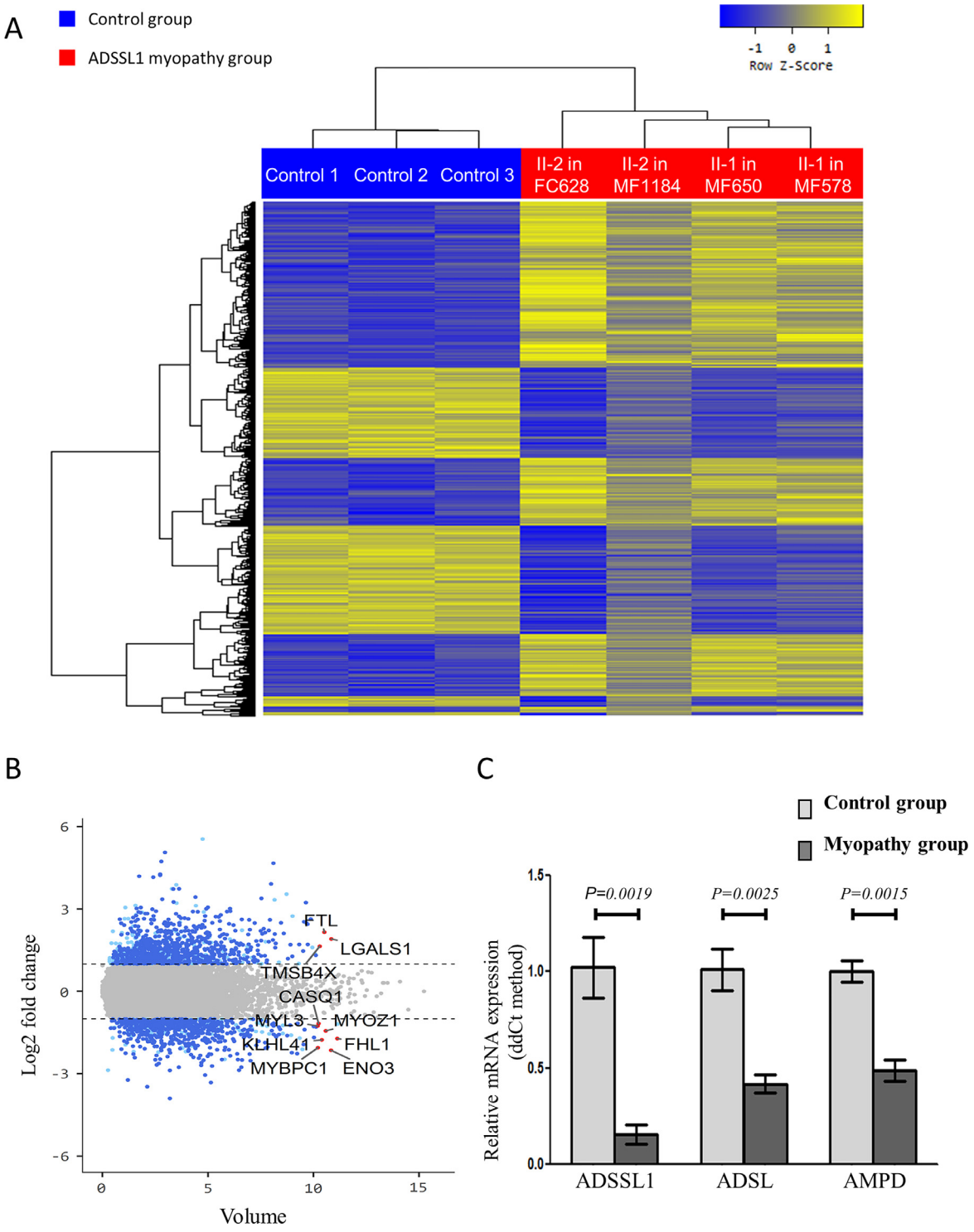

Fig. 1. **Transcriptomic characterization of ADSSL1 myopathy and control groups.** (A) Heat map for hierarchical clustering. The heatmap was generated by R package "plots" using the expression for each gene (rows) and sample (columns). The expression levels of each gene across samples are shown as Z-scores scaled by their FPKM from RNA-seq. The scaled expression values are color coded according to the legend. The dendrogram depicting hierarchical clustering is based on the expression of all genes. (B) Volume plot of differentially regulated genes in myopathy group compared with control group. Dark blue dots indicate significantly differentially expressed transcripts ($|\text{fold change}| \geq 2$, $p < 0.05$) and sky-blue dots indicate differentially expressed transcripts ($|\text{fold change}| \geq 2$). *X* axis: volume = square root (control normalized value [control group] × test normalized value [myopathy group]); Y axis: log2 (Fold Change). (C) Comparison of the 2-ΔΔCT values of ADSSL1, ADSL, and AMPD genes when the muscle samples were analyzed collectively in the healthy control group in relation to myopathy group. Expression of three genes involved in purine nucleotide cycle (ADSSL1, ADSL, and AMPD1) between myopathy and control groups by quantitative real-time polymerase chain reaction. GAPDH transcripts were used as a loading control. Error bars represent standard deviation.

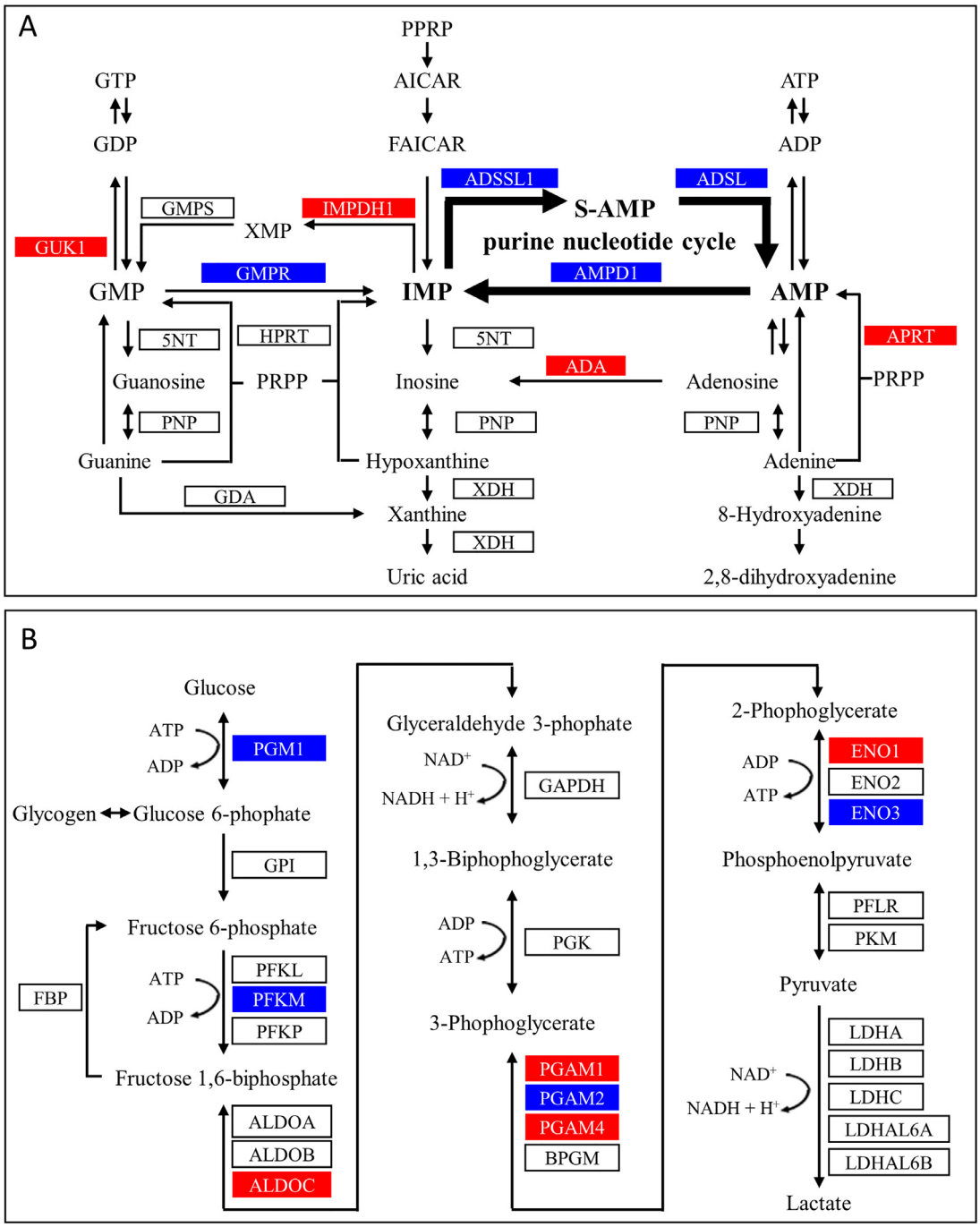

Fig. 2. **Pathways of purine metabolism and glycolysis/gluconeogenesis in skeletal muscle.** (A) Pathways of purine metabolism. (B) Pathways of glycolysis/gluconeogenesis. Genes that are highlighted in blue are significantly downregulated (< 2 fold) in myopathy group. Genes that are highlighted in red are significantly upregulated (> 2 fold) in myopathy group. Bold arrows indicate purine nucleotide cycle. PTPP, phosphoribosyl-pyrophosphate; AICAR, aminoimidazole carboxamide ribotide; FAICAR, formyl-aminoimidazole carboxamide ribotide; IMP, inosine monophosphate; GMP, guanosine monophosphate; GDP, guanosine diphosphate; GTP, guanosine triphosphate; AMP, adenosine monophosphate; S-AMP, adenylosuccinate; ADP, adenosine diphosphate; ATP, adenosine triphosphate; ADSSL1, adenylosuccinate synthetase like 1; ADSL, adenylosuccinate lyase; AMPD1, adenosine monophosphate deaminase 1; 5NT, 5′-nucleotidase; ADA, adenosine deaminase; PNP, purine nucleoside phosphorylase; XDH, xanthine dehydrogenase; HPRT, hypoxanthine-guanine phosphoribosyltransferase; APRT, adenine phosphoribosyltransferase; IMPDH1, inosine monophosphate dehydrogenase 1, GMPS, GMP synthase; GMPR, GMP reductase; GUK1, guanylate kinase 1; PGM1, phosphoglycomutase 1; GPI, glucose phosphate isomerase; PFKL, phosphofructokinase, liver; PFKM, phosphofructokinase, muscle; PFKP, phosphofructokinase, platelet; ALDOA, aldolase, fructose-bisphosphate A; ALDOB, aldolase, fructose-bisphosphate B; ALDOC, aldolase, fructose-bisphosphate C; GAPFH, glyceradehyde-3-phosphate dehydrogenase; PGK, phosphoglycerate kinase; PGAM1, phosphoglycerate mutase 1; PGAM2, phosphoglycerate mutase 2; PGAM4, phosphoglycerate mutase 4; BPGM, bisphosphoglycerate mutase; ENO1, enolase 1; ENO2, enolase 2; ENO3, enolase 3; PKLR, pyruvate kinase isoenzymes R/L; PKM, pyruvate kinase muscle isozyme; LDHA, lactate dehydrogenase A; LDHB, lactate dehydrogenase B; LDHC, lactate dehydrogenase C; LDHAL6A, lactate dehydrogenase A like 6A; LDHAL6B, lactate dehydrogenase A-like 6B.

not show significant increase in serum lactate and ammonia levels (Supplementary Fig. 2).

4. Discussion

RNA-Seq analysis is used as a tool to interrogate global transcriptional changes and to find evidence regarding the biological pathways involved in disease pathogenesis. The present study demonstrated major differences in transcriptional expression level between ADSSL1 myopathy and control groups. One sample from II-2 patient in MF1184 showed a slightly different pattern; however, she was young and had a mild phenotype compared with other patients with ADSSL1 myopathy. Actually, we previously reported that the vastus lateralis muscle was nearly normal in II-2 in MF1184, but were moderately affected in II-2 in FC628 and II-1 in MF578 on muscle MRIs [2–4].

ADSSL1 protein, encoded by the *ADSSL1* gene, is a muscle-specific enzyme with strong expression in skeletal muscle. ADSSL1 is mainly involved in purine nucleotide cycle and catalyzes the initial step in the conversion of inosine monophosphate to adenosine monophosphate [11]. However, the pathogenic mechanism of ADSSL1 myopathy remains unclear. The present analysis by RNA-Seq and qRT-PCR demonstrated downregulation of three genes (*ADSSL1*, *ADSL*, and *AMPD1*) involved in purine nucleotide cycle in the vastus lateralis muscles of patients with ADSSL1 myopathy. Among three genes, the *ADSL* gene is globally expressed in all tissues and alterations in *ADSL* result in a neurologic disorder including encephalopathy, psychomotor delay, autistic behaviors, and seizures [12]. In contrast, the *AMPD1* and *ADSSL1* genes are predominantly expressed in skeletal muscle tissue. A defective *AMPD1* gene results in exercise-induced myopathy including exercise intolerance, muscle pain, and rhabdomyolysis without permanent muscle weakness [13]. This clinical presentation is different from that of ADSSL1 myopathy.

We also focused on muscle energy metabolism, including glycolysis/gluconeogenesis, and lipid metabolism, as ADSSL1 enzyme directly affects purine metabolism and influences the ability of skeletal muscle fibers to maintain energy and adenosine triphosphate concentrations. We presumed that the deficiency of ADSSL1 enzyme is more directly linked to glycolysis/gluconeogenesis pathway than fatty acid degradation pathway. Firstly, purine metabolism can influence glycolysis/gluconeogenesis. Purine nucleotides have a role in maintaining high [ATP]:[ADP] and [ATP]:[AMP] ratios [14]. Therefore, dysfunction of purine nucleotide cycle can change the rate of oxidative phosphorylation and influence glycolysis/gluconeogenesis pathway in skeletal muscles [14]. Secondly, two genes (*PGM1* and *PFKM*), which were downregulated in ADSSL1 myopathy, actually caused glycogen storage disease type XIV and VII, respectively. *PGM1* is globally expressed in most cell types and causes multi-systemic disease including dilated cardiomyopathy, growth retardation, myopathy, hypoglycemia, and hepatopathy [15]. Phosphofructokinase, muscle type (PFKM) enzyme, encoded by *PFKM*, is muscle-specific enzyme. The main clinical presentation of patients with a defective *PFKM* gene includes exercise-induced muscle cramps and weakness, myoglobulinuria, and hemolytic anemia. However, a late-onset form of PFKM deficiency shows slowly progressive myopathy without exercise intolerance [16–18]. This clinical presentation is very similar to that of ADSSL1 myopathy [2–4]. Thirdly, we could not find definite evidence for the connection between ADSSL1 myopathy and fatty acid degradation pathway in the present study. Among transcripts linked to fatty acid degradation pathway, myopathy-related genes were not significantly differentially expressed [1]. Four differentially expressed transcripts have not been reported to be associated with muscle disease.

To find evidence of association between ADSSL1 deficiency and abnormal glycolysis/gluconeogenesis pathway, we performed analysis of muscle fiber type proportions and non-ischemic forearm test. Muscle pathology showed predominance of type I fibers in myopathy group compared to control group. The percentages of type 1 fibers in our control group was similar to previous results (23.3 $\sim$ 45.5%) [19]. However, exercise test demonstrated no significant increase in serum lactate and ammonia levels. This result can be explained by the following factors: first, the patient had distal weakness of upper limbs; second, decreased expression of *AMPD1* gene influenced the result of exercise test. In the conditions of a defective *AMPD1* gene, non-ischemic forearm test showed flat ammonia response curve combined with a reduced, but not absent, lactate response [20].

This study has the critical limitation that it was performed with a limited number of muscle samples from ADSSL1 myopathy patients and control subjects. Secondly, patients with myopathy did not have the same gender, disease duration, and clinical severity. Thirdly, we could not match patients and control subjects based on their age and gender. Lastly, we studied muscle specimens with the same pathogenic variants in *ADSSL1*, which limited the interpretation of our results. However, ADSSL1 myopathy was recently identified in only a few Korean patients. we could not obtain sufficient muscle specimens of healthy subjects because muscle biopsy is an invasive modality. To overcome this limitation, we used only the vastus lateralis muscles of myopathy patients and control subjects. Additionally, we selected patients with ADSSL1 myopathy who had the same pathogenic variants. We selected control subjects with normal serum CK level, normal muscle pathology, and no definite motor weakness.

The present study demonstrated gene expression profiles of skeletal muscle tissues in patients with ADSSL1 myopathy. The heat map for hierarchical clustering results revealed a separation between myopathy and control groups. We identified significant downregulation of three genes (*ADSSL1*, *ADSL*, and *AMPD1*) involved in purine nucleotide cycle and two genes (*PGM1* and *PFKM*) involved in glycolysis/gluconeogenesis pathways. In addition, the data from Gene Expression Atlas show that comparing two significant pathways in this study, similar patterns of

expression can be found in other myopathy patients. Specifically, DMD patients show that *GMPR, ADSSL1* and *PGAM2* genes is significantly downregulated whereas *ENO1* gene is significantly upregulated. DYSF patients show that *ENO1* gene is significantly upregulated.

In conclusion, this is the first study showing altered expression of transcripts in muscle tissues of patients with ADSSL1 myopathy. Our results provide new insight into the pathogenesis of ADSSL1 myopathy.

Acknowledgments

We would like to thank the patients who participated in this study and provided their tissues and/or blood for medical research. This study was supported by a faculty research grant of Yonsei University College of Medicine (6-2016-0153).

Supplementary materials

Supplementary material associated with this article can be found, in the online version, at doi:10.1016/j.nmd.2018.11.003.

References

[1] Bonne G, Rivier F, Hamroun D. The 2018 version of the gene table of monogenic neuromuscular disorders (nuclear genome). Neuromuscul Disord 2017;27:1152–83.
[2] Park HJ, Hong YB, Choi YC, et al. ADSSL1 mutation relevant to autosomal recessive adolescent onset distal myopathy. Ann Neurol 2016;79:231–43.
[3] Park HJ, Lee JE, Choi GS, et al. Electron Microscopy Pathology of ADSSL1 Myopathy. J Clin Neurol 2017;13:105–6.
[4] Park HJ, Shin HY, Kim S, et al. Distal myopathy with ADSSL1 mutations in Korean patients. Neuromuscul Disord 2017;27:465–72.
[5] Trapnell C, Roberts A, Goff L, et al. Differential gene and transcript expression analysis of RNA-seq experiments with TopHat and Cufflinks. Nat Protoc 2012;7:562–78.
[6] Tuch BB, Laborde RR, Xu X, et al. Tumor transcriptome sequencing reveals allelic expression imbalances associated with copy number alterations. PloS One 2010;5:e9317.
[7] Twine NA, Janitz K, Wilkins MR, Janitz M. Whole transcriptome sequencing reveals gene expression and splicing differences in brain regions affected by Alzheimer's disease. PloS One 2011;6:e16266.
[8] Mutryn MF, Brannick EM, Fu W, Lee WR, Abasht B. Characterization of a novel chicken muscle disorder through differential gene expression and pathway analysis using RNA-sequencing. BMC Genom 2015;16:399.
[9] Trapnell C, Pachter L, Salzberg SL. TopHat: discovering splice junctions with RNA-Seq. Bioinformatics 2009;25:1105–11.
[10] Trapnell C, Williams BA, Pertea G, et al. Transcript assembly and quantification by RNA-Seq reveals unannotated transcripts and isoform switching during cell differentiation. Nat Biotechnol 2010;28:511–15.
[11] Sun H, Li N, Wang X, et al. Molecular cloning and characterization of a novel muscle adenylosuccinate synthetase, AdSSL1, from human bone marrow stromal cells. Mol Cell Biochem 2005;269:85–94.
[12] Zikanova M, Skopova V, Hnizda A, Krijt J, Kmoch S. Biochemical and structural analysis of 14 mutant adsl enzyme complexes and correlation to phenotypic heterogeneity of adenylosuccinate lyase deficiency. Hum Mutat 2010;31:445–55.
[13] Gross M. Clinical heterogeneity and molecular mechanisms in inborn muscle AMP deaminase deficiency. J Inherit Metab Dis 1997;20:186–92.
[14] Tornheim K, Lowenstein JM. The purine nucleotide cycle. IV. Interactions with oscillations of the glycolytic pathway in muscle extracts. J Biol Chem 1974;249:3241–7.
[15] Tegtmeyer LC, Rust S, van Scherpenzeel M, et al. Multiple phenotypes in phosphoglucomutase 1 deficiency. N Engl J Med 2014;370:533–42.
[16] Vora S, DiMauro S, Spear D, Harker D, Danon M. Characterization of the enzymatic defect in late-onset muscle phosphofructokinase deficiency. New subtype of glycogen storage disease type VII. J Clin Invest 1987;80:1479.
[17] Sivakumar K, Vasconcelos O, Goldfarb L, Dalakas MC. Late-onset muscle weakness in partial phosphofructokinase deficiency: a unique myopathy with vacuoles, abnormal mitochondria, and absence of the common exon 5/intron 5 junction point mutation. Neurology 1996;46:1337–42.
[18] Malfatti E, Birouk N, Romero NB, et al. Juvenile-onset permanent weakness in muscle phosphofructokinase deficiency. J Neurol Sci 2012;316:173–7.
[19] Johnson MA, Polgar J, Weightman D, Appleton D. Data on the distribution of fibre types in thirty-six human muscles: an autopsy study. J Neurol Sci 1973;18:111–29.
[20] Livingstone C, Chinnery PF, Turnbull DM. The ischaemic lactate-ammonia test. Ann Clin Biochem 2001;38:304–10.